Stability of Rock Riprap for Protection at Toe of Abutments at Flood Plain

JORGE E. PAGÁN-ORTIZ

The results of research conducted in a hydraulic flume to determine the stability of rock riprap protecting abutments located on flood plains are presented. The observed vulnerable zone for rock riprap failure is presented for two abutment types: vertical-wall and spill-through (H:V = 2:1). Equations and velocity multipliers to assist an engineer in determining the stable rock riprap size are presented for the two abutment types. Conditions found to influence the stability of rock riprap are also presented.

Bridge abutments commonly contract the free flow of water in the channel and flood plains through the bridge opening during high flows. During high flow events, the abutments are subject to strong erosive currents that are forced to pass through the bridge opening. These currents undermine the stream bed at the toe of the abutments and beyond. This phenomen, known as local scour at the abutments, in turn causes acceleration of flow deflected by the abutments. The development of a vortex system induced by the obstruction is the principal mechanism for the development of local scour. The strength of the vorticity generated by the deflection is related to the depth of flow, abutment depth and shape, alignment of the abutment with respect to the flow, size of bed material, rate of bed material transportation, and ice or drift accumulation.

Laboratory measurements indicate that average point velocities away from the abutment area are not influenced by the abutment's presence. Consequently, scour at abutments is considered a local phenomenum that is not significantly related to the overall geometry of the flow (*1*).

A common method for protecting the stream bed from erosive currents is that of placing a rock riprap apron. To determine the size of rock riprap needed to prevent local scouring at abutments, it is necessary to study the stability of the rock as it is exposed to the erosive currents in the channel and flood plain.

LITERATURE REVIEW

The FHWA procedure for determining the rock riprap size to protect abutments from scouring is presented in the Hydraulic Engineering Circular (HEC) 11, entitled *Design of Riprap Revetment* (*2*). The rock riprap size is determined using the following equation:

$$D_{50} = \frac{0.001 * V_a^3}{d_{avg}^{0.05} * K_1^{1.5}} \quad (1)$$

Federal Highway Administration, Bridge Division, Hydraulics and Geotechnical Branch, 400 Seventh Street, S.W., Washington, D.C. 20590.

where

D_{50} = median rock riprap particle size (ft),
V_a = average velocity in the main channel at the constricted section (ft/sec),
d_{avg} = average flow depth in the main flow channel at the constricted section (ft), and
K_1 = bank angle/rock angle factor defined as

$$K_1 = \left(1 - \frac{\sin^2\theta}{\sin^2\phi}\right)^{0.5} \quad (2)$$

where θ is the bank angle with the horizontal, and ϕ is the rock riprap material's angle of repose.

The rock size (D_{50}) computed from Equation 1 must be multiplied by a correction factor C because when the equation was developed, information on velocities in the vicinity of bridge abutments was not available. The factor C is computed as follows:

$$C = C_{sg} * C_{sf} \quad (3)$$

where

$$C_{sg} = \frac{2.12}{(S_s - 1)^{1.5}} \quad (4)$$

and

$$C_{sf} = \left(\frac{SF}{1.2}\right)^{1.5} \quad (5)$$

where

C_{sg} = correction factor for specific gravities other than 2.65,
C_{sf} = correction factor for stability,
SF = stability factor ranging from 1.6 to 2.0 for turbulent flow at the bridge abutment, and
S_s = specific gravity of the rock riprap.

Many researchers have developed equations based on average velocity that relate the critical conditions affecting stability. Isbash (*3*) presented an equation that can be expressed as

$$N_{sc} = E^2 * 2 \quad (6)$$

where N_{sc} is the sediment number representing the ratio of approach flow inertial energy at critical conditions to the

stabilizing potential created by the submerged rock weight (*4*).

For loose stone lying on top of the fill, N_{sc} is expressed as

$$N_{sc} = \frac{V^2}{g * D_{50} * (SG - 1)} \tag{7}$$

where

V = flow velocity that will remove the loose stones (ft/sec),
D_{50} = characteristic median rock size (ft),
SG = specific gravity of the rock,
g = gravitational acceleration (32.2 ft/sec^2), and
E = 0.86 for loose stone lying on top of the fill.

For stones deposited into flowing water that roll (because of the force of water acting over them) until they find a "seat" and a support, $E = 1.2$.

Rearranging Equation 7 in terms of D_{50} for $E = 1.2$, we obtain

$$D_{50} = \frac{0.347 * V^2}{g * (SG - 1)} \tag{8}$$

Equation 8 is a rearranged form of the Isbash equation.

Neill established a relation for "first displacement" of uniform graded gravel based on uniform parameters (*5*). The following expresses a conservative design curve:

$$N_{sc} = 2.50 * \left(\frac{D_g}{d}\right)^{-0.20} \tag{9}$$

where D_g is the characteristic rock size on the approach flow bed (in feet) and d is the depth of the approach flow (in feet).

Neill compared his results with those of Mavis, Ho, and Tu; Schaffernak; Meyer-Peter and Müller; and Linnton Hydraulics Laboratory and found good agreement. Parola conducted experiments using Neill's criteria for first displacement and found good agreement too (*4*).

Pagán (*6*) developed the following regression equation for an average sediment number design curve based on Neill's and Parola's experiments for undisturbed flow:

$$N_{sc} = 2.58 * \left(\frac{D_g}{d}\right)^{-0.27} \tag{10}$$

The average design curve represented by Equation 10 will be compared with an average curve to be developed from a series of parameters that characterize the disturbed flow.

Figure 1 shows the sediment number curve, N_{sc}, based on Neill's and Parola's experiments for undisturbed flow—no obstruction to the free flow of water.

FRAMEWORK OF EXPERIMENTS

The parameters that characterize the disturbed flow are

- V_{cc}—average velocity of the contracted flow at observed incipient motion of the rock at the contraction (ft/sec);
- d_{cc}—average depth of the contracted flow at observed incipient motion of rock at the contraction (ft);
- W_a—width of the approach flow (ft);
- W_{t-c}—width of the contraction (ft);
- D_{50}—characteristic median rock size on the contraction flow bed (ft);
- AS—factor associated with the abutment shape;
- K—roughness of the bed upstream;
- K_s—roughness of the bed surrounding the obstruction;

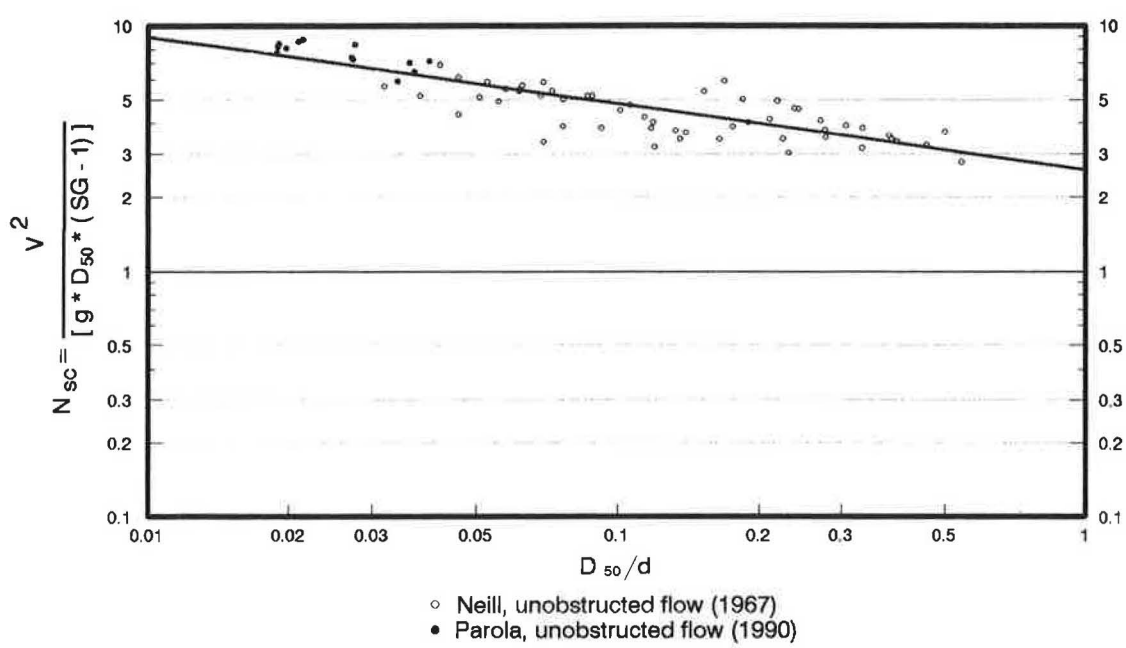

FIGURE 1 Sediment number curve for unobstructed flow.

- g—gravitational acceleration (32.2 ft/sec^2);
- ρ—fluid density (slug/ft^3);
- ρ_s—rock density (slug/ft^3); and
- μ—dynamic viscosity of fluid (slug/ft-sec).

The effect of displacement due to leaching of fines through the armored apron of gravel in the observation area near the toe of the abutment and flood plain was not studied. The size of the bed material (D_{50}) in the obstructed area and the roughness in the vicinity of the obstruction (K_s) are dependent variables. For the purpose of the experiments, K_s was assumed to be adequately represented by D_{50}.

The characteristic parameters can be arranged into a functional equation that describes the critical condition for the initial motion of the rock within the observation area as follows:

$$0 = f(W_a, W_{t-c}, d_{cc}, D_{50}, V_{cc}, AS, K, g, \rho, \rho_s, \mu) \quad (11)$$

The parameter g must appear in combination with ρ and ρ_s as follows:

$$\gamma = g * (\rho_s - \rho) \quad (12)$$

Combining Equations 11 and 12 in a nondimensional form yields

$$N_{sc} = f\left(V_{cc} * \frac{D}{\nu}, \frac{\rho_s}{\rho}, \frac{d_{cc}}{W_{t-c}}, \frac{D_{50}}{d_{cc}}, AS, \frac{W_a}{W_{t-c}}, K\right) \quad (13)$$

where ν equals μ/ρ and D is characteristic rock size (assumed to be adequately represented by D_{50}).

Yalin stated that (ρ_s/ρ) "can be important only with regard to the properties associated with the 'ballistics' of an individual grain. In case of highly turbulent flows needed to cause the initial motion of the rock protection, the influence of the obstruction particle Reynolds' number—effect of viscosity relative to inertia, $V_{cc} * (D/\nu)$—was considered to be negligible because it was greater than 10^3, which is well beyond the range that Shields and other researchers found to be no longer a factor.

Therefore, by applying the preceding considerations and confining the research to subcritical flow, the effect of (ρ_s/ρ) and $[V_{cc} * (D/\nu)]$ can be discounted. Thus, Equation 13 can be reduced as follows:

$$N_{sc} = f\left(\frac{d_{cc}}{W_{t-c}}, \frac{D_{50}}{d_{cc}}, AS, \frac{W_a}{W_{t-c}}, K\right) \quad (14)$$

By using the contracted velocity in N_{sc}, the effect of d_{cc}/W_{t-c}, W_a/W_{t-c}, and K are negligible. Thus, Equation 14 reduces to

$$N_{sc} = f\left(\frac{D_{50}}{d_{cc}}, AS\right) \quad (15)$$

Equation 14 provides the framework used to determine the stability of rock riprap to protect the toe of an abutment at the flood plain. The quantity N_{sc} is defined in Equation 6. The parameter D_{50}/d_{cc} represents the relative roughness of the contracted flow.

Experimental Model

Tow small-scaled abutment models—vertical-wall and spill-through—were used to study the impact of the abutments on time-averaged contraction velocities and the stability of gravel placed around the toe of the abutment and flood plain. The length of the abutment was varied to investigate the effect of the contraction to the flow on the flood plain. For the vertical-wall abutment, the length ranged from 5 to 20 in.; for the spill-through model, the length ranged from 25 to 40 in. The total widths of the vertical-wall and spill-through abutments were 6 and 46 in., respectively. Flow depths ranged from 1.84 to 10.5 in.

Observation Area

An observation area was defined in the hydraulic flume for each abutment model to visualize the failure of gravel for a given flow. These areas are illustrated in Figures 2 and 3.

Gravel Placement

Two sizes of gravel were used in the experiments: D_{50} = 0.30 in. and D_{50} = 0.40 in. The gravel was angular particles that

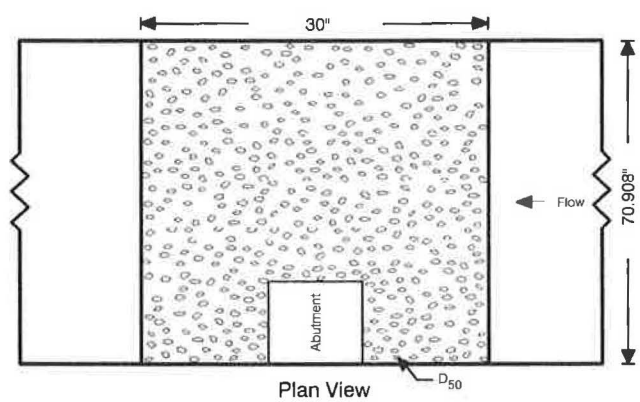

FIGURE 2 Observation area for vertical-wall abutment.

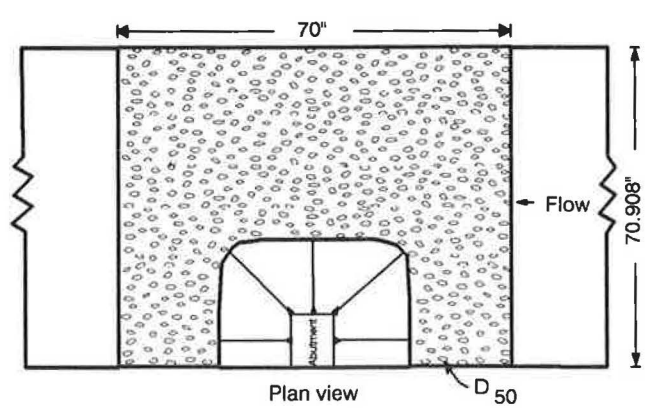

FIGURE 3 Observation area for spill-through abutment.

passed on sieve and were retained on the next standard size so they were intended to be uniform in size. A grain size distribution analysis was run on several samples of the bin of materials used in the experiments. On the basis of these samples, the gravel had a geometric standard deviation of $(D_{84}/D_{16})^{1/2}$ of 1.08 and 1.10 for D_{50} = 0.30 and 0.40 in., respectively.

The gravel was placed in the observation area to a depth of 1.5 in. in three nonuniform layers. The intermediate layer was spray-painted red to help visualize the failure or motion of the upper gravel layer. Figures 4 and 5 illustrate a typical gravel setup for each abutment model. Gradation and layer thickness were not variables in these experiments.

Experimental Procedure

The experimental procedure for each run was as follows:

1. The discharge was set to a constant.
2. The tailgate was raised to develop a velocity past the observation section slightly below the expected incipient velocity of the rock riprap failure.
3. The tailgate was gradually lowered until a discernible patch of surface rock moved in the observation section. This was determined by looking for a visible section of the colored underlying layer of rock.
4. The flow and the tailgate setting were then held constant while a grid of depth and velocity measurements was taken.

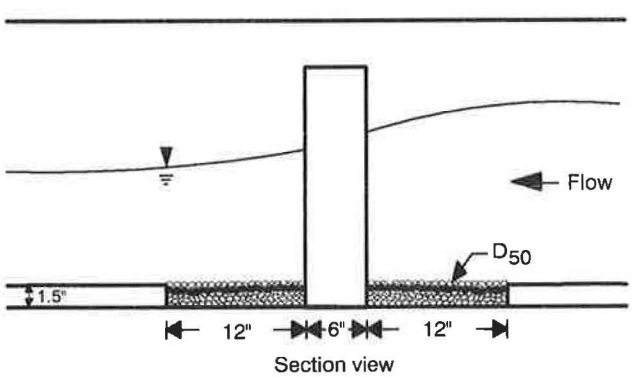

FIGURE 4 Section view of gravel setup for vertical-wall abutment.

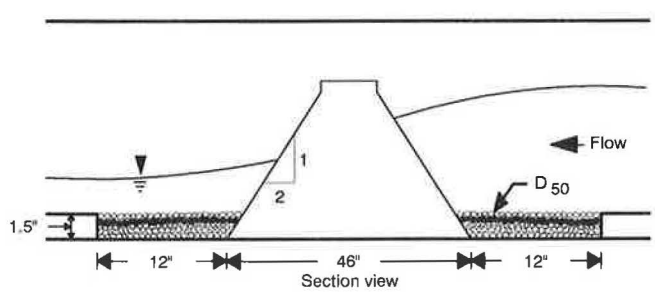

FIGURE 5 Section view of gravel setup for spill-through abutment.

This generally took about 1½ hr. Very few additional particles moved during this data collection period, so it was thought that longer run times would not have changed the results.

Some reviewers implied that longer run times should have been used. The shorter run times were considered appropriate because these were essentially incipient motion experiments rather than depth-of-scour experiments. In hindsight, it would have been useful to run a few experiments at a slightly lower velocity for a long duration (say, 72 hr) to determine whether longer duration tests would have significantly changed the results.

EXPERIMENTAL RESULTS

Independent experiments were conducted with each abutment model to determine the vulnerable zone for the gravel failure within the observation area at different discharges and flow depths. An initial zone of failure thus was identified for each model.

Previous researchers have demonstrated that the scour hole pattern in an unprotected channel and flood plain being obstructed by either a vertical-wall or spill-through abutment normal to the flow occurs at the upstream corner of the abutment (*7*). Pagán (*6*) demonstrated that the failure zone in an armored flood plain surrounding the abutment normal to the flow is a function of the abutment shape.

For the vertical-wall abutment the initial failure zone was consistently observed at the upstream corner of the abutment in the armored flood plain (Figure 6). The zone then expands downstream toward the abutment and away from it with time and increase in discharge.

For the spill-through abutment model, the initial failure zone was consistently observed at the downstream radius of the model just away from its toe (Figure 7). The zone then expands downstream and upstream toward the toe of the abutment and away from it into the flood plain with time and increase in discharge.

Velocity-Based Criteria

Three equally spaced average point velocities were measured within the contraction zone. For the smooth bed experiments

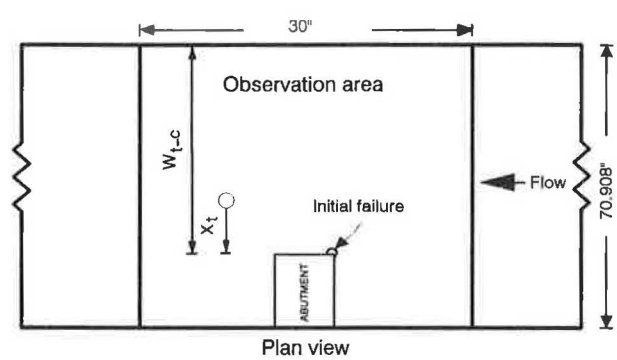

FIGURE 6 Location of initial failure zone for vertical-wall abutment.

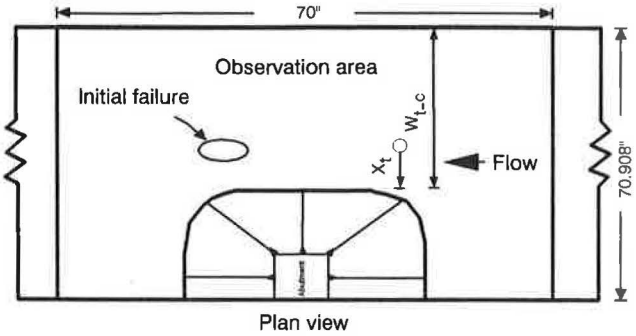

FIGURE 7 Location of initial failure zone for spill-through abutment.

(no gravel placed within the observation area), it was learned that the readings of average point velocities near the face of the abutment parallel to the flow were severely affected by the flow turbulence. Consequently, low velocity readings were measured near the face of the abutment. The same result was obtained in the obstructed flow experiments (gravel placed in the observation area). However, the gravel was failing at the upstream corner of the vertical-wall abutment (Figure 6) and downstream near the toe for the spill-through abutment (Figure 7). Thus, although the flow turbulence affected the velocity readings near the abutment models, that velocity must be much higher that those measured during the experiments to cause the initial motion of the gravel near the toe of the abutment models.

An indirect method to obtain the velocity near the face of the abutment at which the incipient motion of the gravel is observed is to compare the velocity measured with the abutment constricting the free flow, plotting those velocities in terms of the sediment number (N_{sc}), and comparing the plot to that shown in Figure 1.

Vertical-Wall Abutment

The vulnerable zone for incipient motion for this abutment shape was observed at the upstream corner of the abutment (Figure 6). The separation of flow created by the contraction of the abutment shape caused a strong turbulence, particularly for deeper flows. With the flow depth and velocity at the approach and for a computed discharge at the approach representing the design discharge, the velocity and flow depth were computed at the contraction of the abutment in the flood plain using Bernoulli's energy equation without elevation terms and the continuity equation. The energy equation is as follows:

$$\frac{V_{am}^2}{2 * g} + d_a = \frac{V_{cc}^2}{2 * g} + d_{cc} + h_L \tag{16}$$

where

V_{am} = measured average point velocity at the approach (ft/sec),
d_a = average measured depth at the approach (ft),
V_{cc} = computed average point velocity at the contraction for disturbed flow (ft/sec),
d_{cc} = average computed depth at the contraction for obstructed flow (ft), and
h_L = energy losses (assumed to be negligible) (ft).

The continuity equation is

$$Q_{cc} = V_{cc} * W_{t-c} * d_{cc} \tag{17}$$

where Q_{cc} is the computed discharge (in cubic feet per second), and W_{t-c} is the horizontal distance from the toe of the abutment to the channel boundary (in feet).

Using Equation 7, N_{sc} was computed for V_{cc}. The values of N_{sc} were plotted against the D_{50}/d_{cc} ratio. Figure 8 shows a plot of the individual computed sediment number curve for the vertical-wall abutment model for D_{50} = 0.30 and 0.40 in. for obstructed flow.

Figure 8 also shows that the curves for the two gravel sizes, which were derived by regression, were close to one curve and almost parallel to the unobstructed flow curve. The velocity, V_{cc}, is the computed average contracted velocity in the opening for the obstructed flow, but observed failure is for any discernible area of particular movement in that opening.

Figure 9 shows the combined sediment number curve for the two gravel sizes. This plot reveals that the slope of the combined curve follows that of the unobstructed flow curve. For the gravel to fail at the toe of the abutment upstream of the constriction, the local effective velocity must have been close to that which would have caused failure for the unobstructed flow.

Flow at the end of the abutment where the initial failure of rock riprap usually occurs was highly rotational and difficult to quantify with the electromagnetic probe sensor, the instrument available for this study. A so-called local effective velocity was defined as the velocity that would have moved the rock in unobstructed flow.

To determine the stable size of rock riprap, Equation 7 should be rearranged as follows:

$$D_{50} = \frac{V_{cc}^2}{g * N_{sc} * (SG - 1)} \tag{18}$$

By regression analysis of the combined sediment number curve (Figure 9), N_{sc} is obtained as

$$N_{sc} = 0.94 * \left(\frac{D_{50}}{d_{cc}}\right)^{-0.23} \tag{19}$$

Substituting Equation 19 into Equation 18 yields

$$D_{50} = \frac{1.0836 * V_{cc}^{2.598}}{g^{1.299} * d_{cc}^{0.299} * (SG - 1)^{1.299}} \tag{20}$$

Although Equation 20 is not dimensionless as written, it is dimensionally homogeneous—that is, it can be reduced to the same units on both sides. It can be used with either SI or English units as long as consistent units are used in all terms.

Figure 10 presents a plot of V_{cp}/V_{cc} versus X_t/W_{t-c}. At X_t/W_{t-c} = 0, and for 95 percent of the computations, the ratio V_{cp}/V_{cc} fell near 2.0. At X_t/W_{t-c} = 0, and for 5 percent of the computations, the ratio reached 2.304. V_{cp}/V_{cc} repre-

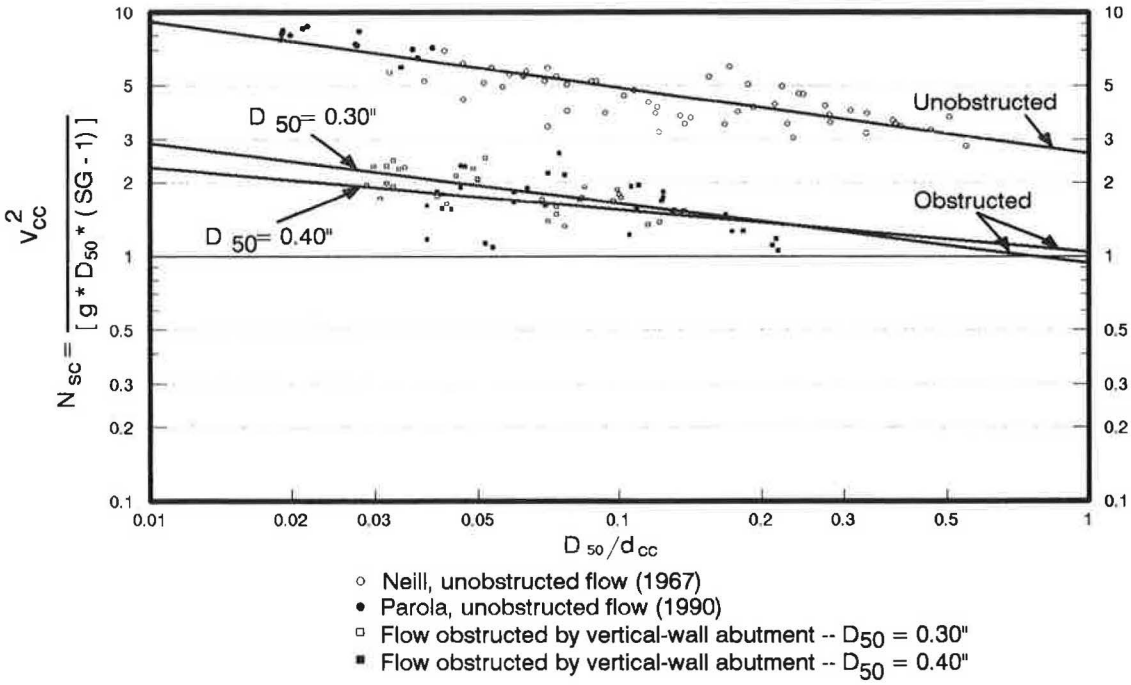

FIGURE 8 Individual sediment number curve for vertical-wall abutment.

sents the effective computed local velocity (near the abutment face at which the rock failed) to the average computed contracted velocity in the flood plain within the contraction. The ratio of V_{cp}/V_{cc} also represents the indirect method—or "simple multiplier"—that should be applied to the average computed contracted velocity in the contraction within the flood plain to obtain the velocity near the abutment face that caused the gravel's incipient motion.

V_{cp} is the computed average point velocity at the contraction for undisturbed flow, in feet per second. V_{cc} is the average computed point velocity, feet per second, at various distances, X_t, from the toe of the abutment for disturbed flow. W_{t-c} is the horizontal distance from the toe of the abutment to the channel boundary, in feet.

The effective velocity had no resemblance to what actually occurred around the abutment, but it was a convenient pa-

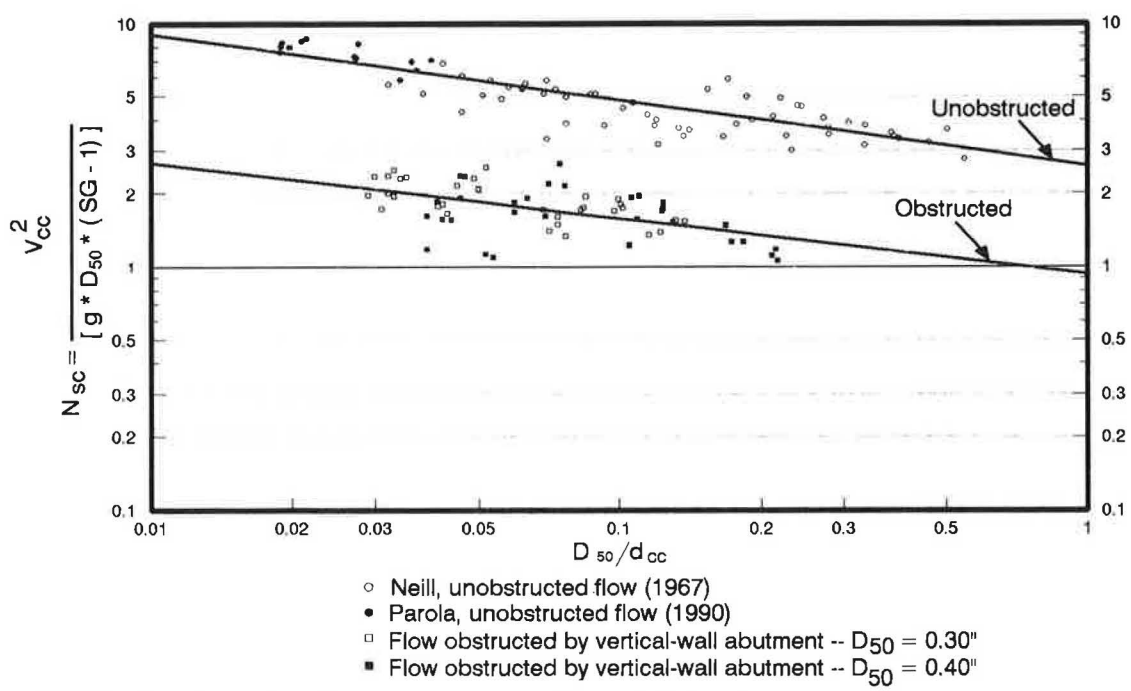

FIGURE 9 Combined sediment number curve for vertical-wall abutment.

rameter to use in developing a simple multiplier (V_{cp}/V_{cc}) for the velocity term in the rearranged Isbash equation—Equation 8. The velocity term within Equation 8 can be multiplied by 2.0 to compute the rock riprap size for the vertical-wall abutment model.

The discharge was increased 1.7 times the discharge that caused the incipient motion of the gravel to observe the extent of the failure zone. The multiplier, 1.7, is suggested on FHWA publication HEC-18 (*8*) to approximate Q_{500} from Q_{100}. This demonstrated that the rock riprap apron should be extended along the entire length of the abutment, both upstream and downstream, and to the parallel face of the abutment to the flow.

Figure 10 also illustrates that the velocity amplification decays rapidly with distance from the toe of the abutment—the effect of the abutment diminished quickly with distance from the abutment. Therefore, it would be reasonable to limit the rock riprap apron to a relative small portion of the constriction. However, additional data analysis is necessary to determine the extent of the rock riprap apron.

Spill-Through Abutment

The observed vulnerable zone for incipient motion for this model was observed downstream of the contraction near the toe of the abutment (Figure 7). The acceleration of flow through the slope of the spill face of the abutment parallel to the flow and the turbulence developed at the vena contracta—the most contracted section of a stream jet—are believed to have influenced the gravel failure at the mentioned zone. With the flow depth and velocity measured at the approach and for a computed discharge at the approach representing the design discharge, the velocity and flow depth were also computed at the contraction of the abutment in the flood plain using Equations 16 and 17.

Using Equation 7, N_{sc} was computed with V_{cc}. The values of N_{sc} were plotted versus the D_{50}/d_{cc} ratio. Figure 11 shows a plot of the individual computed sediment numbers curve for spill-through abutment for D_{50} = 0.30 and 0.40 in. for obstructed flow.

Because of the adverse slope obtained by regression analysis and the insufficient data at D_{50}/d_{cc} ratio smaller than 0.03, an average N_{sc} of 2.09 and 1.67 was taken for D_{50} = 0.30 and 0.40 in., respectively. A combined sediment number curve was obtained by averaging all the computed N_{sc} values for the two gravel sizes used during the experiments (Figure 12). As a result, the average value of N_{sc} was found to be 1.87. Although the scatter of data on the vertical wall and spill-through experiments is similar, the effect of D_{50}/d_{cc} was found to be less significant for the spill-through abutment.

Figure 12 indicates that for the spill-through model, depth is an important factor in determining the stability of the rock riprap when compared with the unobstructed flow curve. This figure also indicates that for the spill-through abutment, the velocity that caused the incipient motion of the gravel in the flood plain near the toe of the abutment should have been at least that for the unobstructed flow.

Therefore, to determine the stable size of rock riprap, Equation 7 should be used as follows:

$$D_{50} = \frac{0.535 * V_{cc}^2}{g * (SG - 1)} \tag{21}$$

Figure 13 presents a plot of V_{cp}/V_{cc} versus X_t/W_{t-c}. The velocity ratio, V_{cp}/V_{cc}, and V_{cc}, V_{cp}, X_t, and W_{t-c} remain as previously defined. At X_t/W_{t-c} = 0, and for 97 percent of the computations, the ratio of V_{cp}/V_{cc} fell near 2.0. At

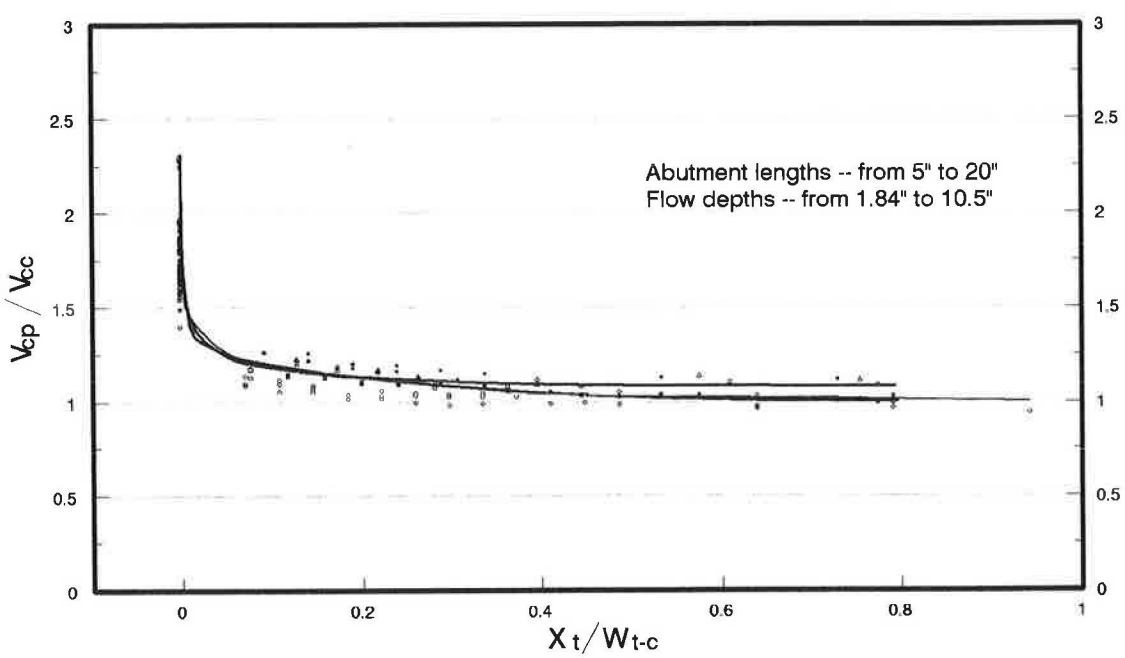

FIGURE 10 Point velocity ratio for vertical-wall abutment.

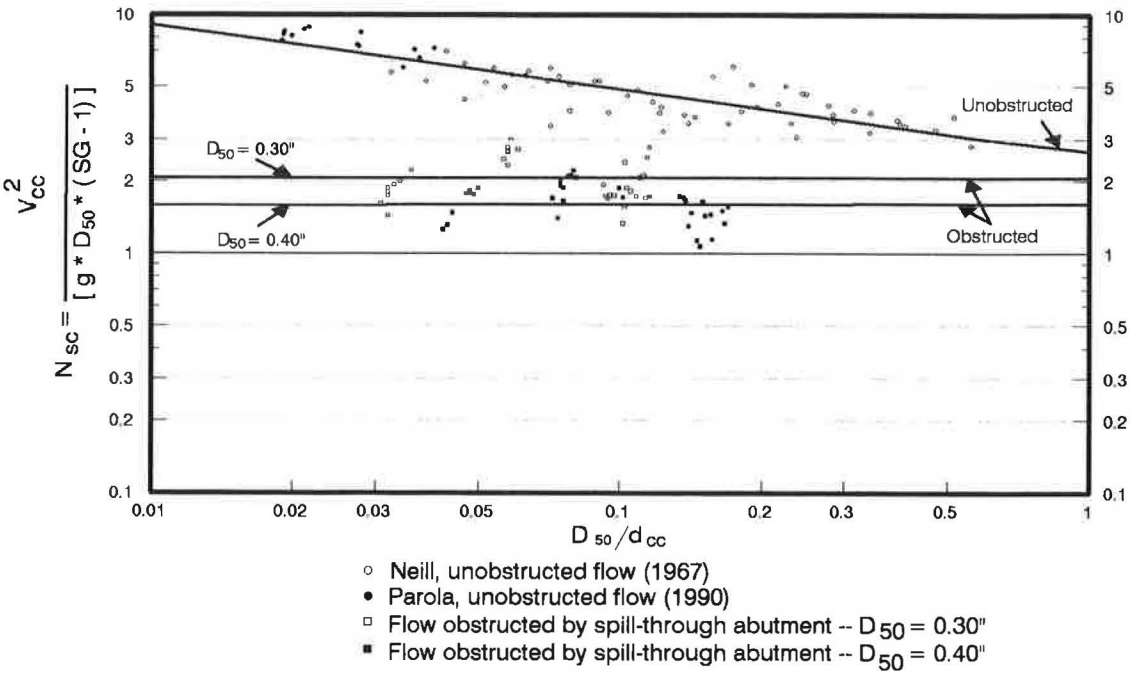

FIGURE 11 Individual sediment number curve for spill-through abutment.

$X_t/W_{t-c} = 0$, and for 3 percent of the computations, the ratio of V_{cp}/V_{cc} reached 2.135.

The ratio of V_{cp}/V_{cc} also represents the indirect method—or "simple multiplier"—that should be applied to the averaged computed contracted velocity in the contraction within the flood plain to obtain the velocity near the abutment face that caused the incipient motion of the gravel.

The local effective velocity had no resemblance to what actually occurred around the abutment, but it was a convenient parameter to use in developing a simple multiplier (V_{cp}/V_{cc}) for the velocity term in the rearranged Isbash equation—Equation 8. Similarly to vertical-wall abutment, the velocity term in the rearranged Isbash equation can be multiplied by 2.0 to compute the rock riprap size for the spill-through abutment.

As with the vertical-wall abutment model, the discharge was also increased by 1.7 times the discharge that caused the incipient motion of the gravel to observe the extent of the

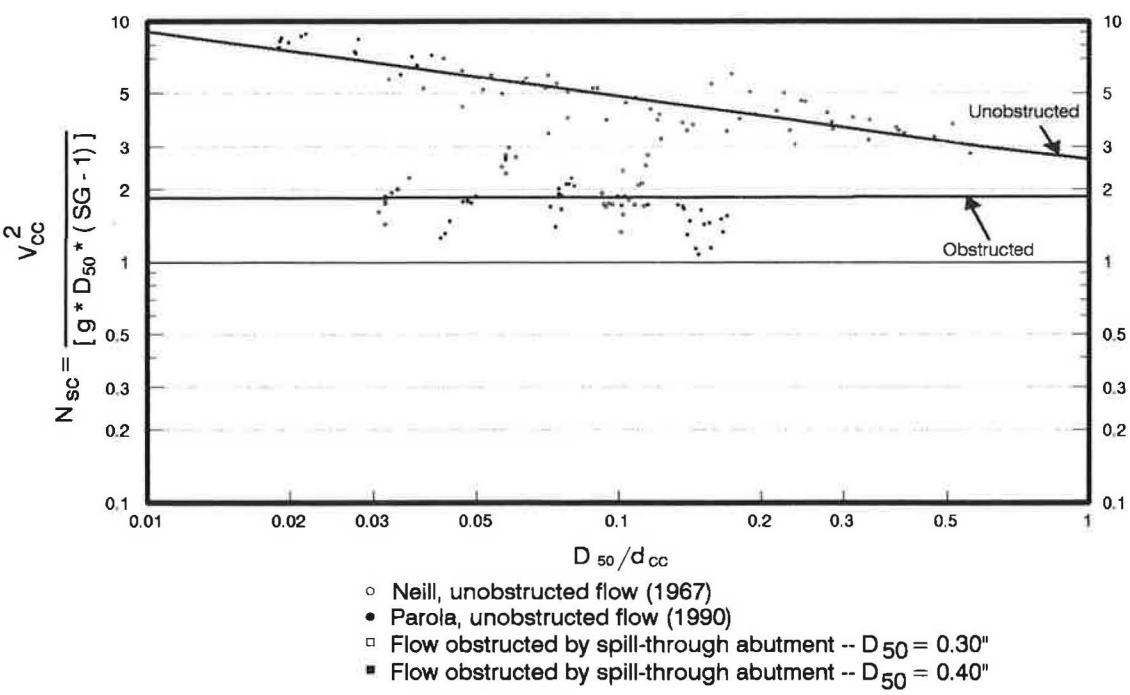

FIGURE 12 Combined sediment number curve for spill-through abutment.

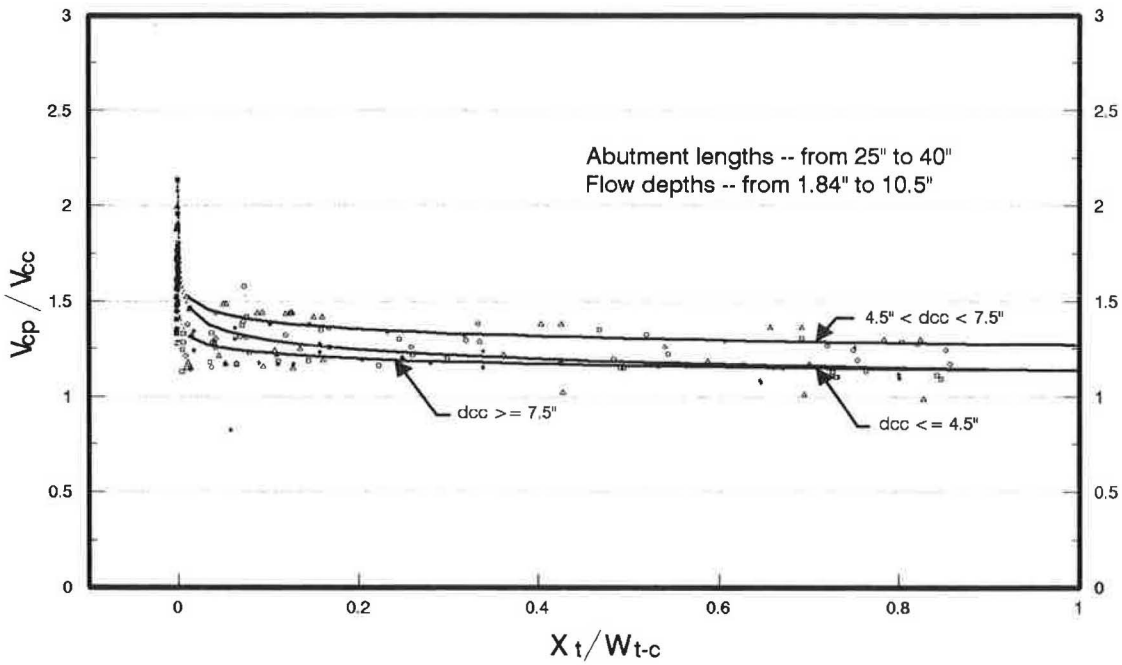

FIGURE 13 Point velocity ratio for spill-through abutment.

failure zone. This demonstrated that the rock riprap apron should be extended along the entire length of the abutment, both upstream and downstream, and to the parallel face of the abutment to the flow.

Figure 13 illustrates that the velocity amplification decays rapidly with distance from the toe of the abutment and that the effect of the abutment diminishes quickly with distance from the abutment. Also, the effect of the abutment occurs in a small portion of the contracted area. Therefore, as with the vertical-wall abutment, it would be reasonable to limit the rock riprap apron to a relatively small portion of the constriction. Again, however, more data analysis is needed to determine the extent of the rock riprap apron for this model.

Some of the preliminary results of this research have been included in HEC-18. It is anticipated that a more complete treatment of this topic will be in updates of HEC-18.

CONCLUSIONS

The location for the most critical failure zone on an abutment encroaching the free flow of water on an armored flood plain depends on the abutment shape. For the vertical-wall abutment model, the critical failure zone occurs at the upstream corner of the abutment and expands downstream toward the abutment and away from the toe with time and increase in discharge. For the spill-through model, the critical failure zone is located downstream of the contraction near the toe and "grows" downstream and upstream of the constriction, expanding to the toe and away from the abutment.

The turbulence of flow and vorticity generated near the face of the abutment are the causes of rock riprap failure. The velocities diminish in intensity and stabilize as distance from the toe of the abutment increases.

Equation 20 can be used to determine a stable rock riprap size to protect the toe of the vertical-wall abutment. Equation 21 can be used for spill-through abutment (note that the use of these equations is limited to abutment encroachments up to 28 percent onto the flood plain for vertical-wall shapes and 56 percent for spill-through shapes—without counting the dimension of the main channel).

The recommended rock riprap thickness should be equivalent to two times D_{50}.

The average velocity in the flood plain within the constricted section should be used in Equations 20 and 21.

The velocity multipliers found in this research for the vertical-wall and spill-through abutments, respectively, can be applied to the velocity term in the Isbash equation for sizing a stable rock riprap size for abutment protection.

Further data analysis is needed to determine the extension of the rock riprap apron for both vertical-wall and spill-through abutments, and further research is needed to investigate the effects of

- A greater encroachment onto the flood plain on the stability of the rock riprap;
- The abutments in a skew to the flow; and
- The main channel in the stability of the rock riprap.

REFERENCES

1. H. K. Liu, F. M. Chang, M. M. Skinner. *Effect of Bridge Constriction on Scour and Backwater*. Feb. 1961.
2. S. A. Brown and E. S. Clyde. *Design of Riprap Revetment*. Hydraulic Engineering Circular 11. FHWA, U.S. Department of Transportation, Washington, D.C., March 1989.
3. S. V. Isbash. Construction of Dams by Depositing Rock in Running Water. *Communication 3, 2nd Congress on Large Dams*, Washington, D.C., 1936.

4. A. Parola, Jr. *The Stability of Riprap Used To Protect Bridge Piers*. Ph.D. dissertation. Pennsylvania State University, State College, May 1990.
5. C. R. Neill and M. S. Yalin. Quantitative Definition of Beginning of Bed Movement. *Journal of the Hydraulics Division*, ASCE, Vol. 95, No. HY1, Jan. 1969.
6. J. E. Pagán-Ortiz. *Stability of Rock Riprap for Protection at the Toe of Abutments Located at the Flood Plain*. M.S. thesis. The George Washington University, Washington, D.C., 1990.
7. *HRB Research Report 13-B: Scour Around Bridges*. HRB, National Research Council, Washington, D.C., 1951.
8. E. V. Richardson, L. J. Harrison, and S. R. Davis. *Evaluating Scour at Bridges*. Hydraulic Engineering Circular 18. FHWA, U.S. Department of Transportation, Washington, D.C., Feb. 1991.